The quest to detect Gravitational Waves from Core-Collapse Supernovae

arXiv:1908.03584 [astro-ph.HE]
(submitted to PRD)

Marek Szczepańczyk
(for the LIGO Scientific Collaboration and the Virgo Collaboration)

4M-COCOS
Fukuoka, 2019.10.23

Outline

- Targeted SNe and on-source window calculation
- Available data and methodology
- Results:
  - Loudest events
  - Detection efficiencies
  - Model exclusion statements
  - GW energy constraints

Targeted CCSNe

- Observing Runs:
  - O1: Sep 2015 – Jan 2016
  - O2: Nov 2016 – Aug 2017
- Surveys: ASAS-SN, DLT40, Gaia, ASRAS, TNS, OSC, CBAT
- **Selection criteria**:
  - Distance less than ~20 Mpc
  - On-source window well identified (order of maximum few days)
  - Sufficient amount of coincident data
- **9 CCSNe considered and 5 passed the selection criteria**: SN 2015as, SN 2016B, SN 2016X, SN 2017eaw and SN 2017gax.
- 4 CCSNe did not pass selection criteria:
  - SN 2016C (type-IIP, 20.1 Mpc) and SN 2017ein (type-Ic, 11.2 Mpc) – not enough GW data was available
  - SN 2017aym (Gaia17aks, type-IIP, 26.4 Mpc) and SN 2017bzb (type-II, 13.9 Mpc) – no on-source window could be sufficiently constrained

Targeted CCSNe

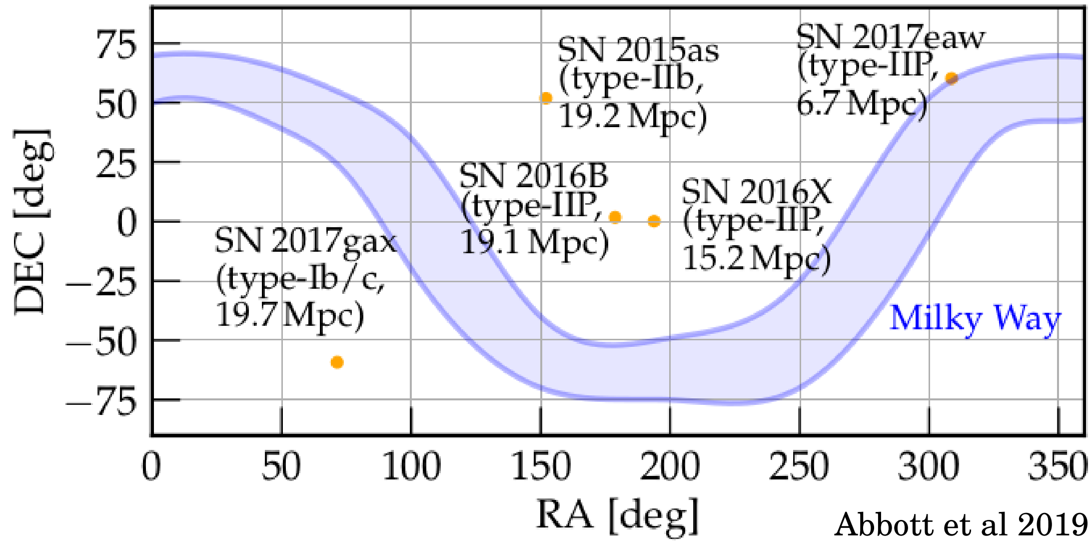

Abbott et al 2019

- **SN 2015as**: type-IIb, 19.2 Mpc, progenitor star is either main sequence 15 $M_\odot$ star or Wolf-Rayet 20 $M_\odot$ star, ejecta 1.1-2.2 $M_\odot$
- **SN 2016B**: type-IIP, 18.6 Mpc, red supergiant
- **SN 2016X**: type-IIP, 15.2 Mpc, >19 $M_\odot$ red supergiant, radius 930 $R_\odot$
- **SN 2017eaw**: type-IIP, 6.7 Mpc, 13 $M_\odot$ red supergiant, radius 4000 $R_\odot$
- **SN 2017gax**: type-Ib/c, 19.7 Mpc, little is known about the progenitor star

On-source window calculations

- **On-source window – period [t_1, t_2]** when we expect to find the GW transient
- t_{disc} – discovery time, upper bound of t_2
- t_{Null} – last observation of a host galaxy without a supernova present
- Δt_{SB} – time between the moment of explosion and shock breakout (few hours to few days)
- Calculations:
  - **Early observation method** – applied when t_{disc} - t_{Null} is of order a few days, the supernova type is known, and the progenitor star is inferred (SN 2015as, SN 2016B, SN 2016X and SN 2017gax)
  - **Expanding photosphere method** – otherwise, multi-band photometry is used to extrapolate backwards in time (SN 2017eaw).

Available data

Run	Detectors	Run Period	Duty Factors	Coin. Duty Factor
O1	H1,L1	2015.09.12–2016.01.19	49.5% (H1), 42.4% (L1)	31.4% (H1L1)
O2	H1,L1	2016.11.30–2017.08.25	65.4% (H1), 63.6% (L1)	49.0% (H1L1)
O2	H1,L1,V1	2017.08.01–2017.08.25	77.7% (H1), 79.2% (L1), 85.1% (V1)	62.0% (H1L1V1)

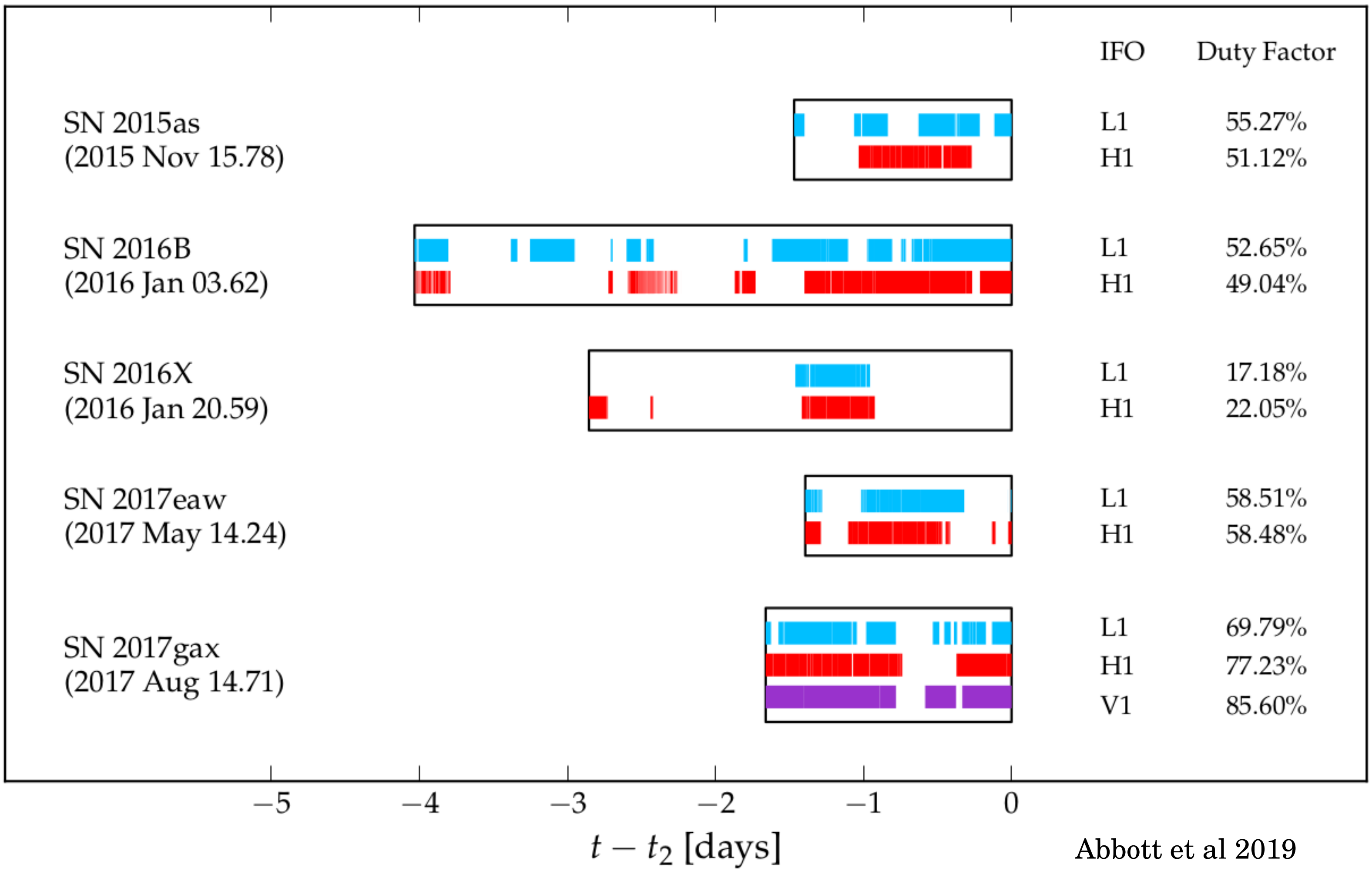

Abbott et al 2019

Detectors sensitivities

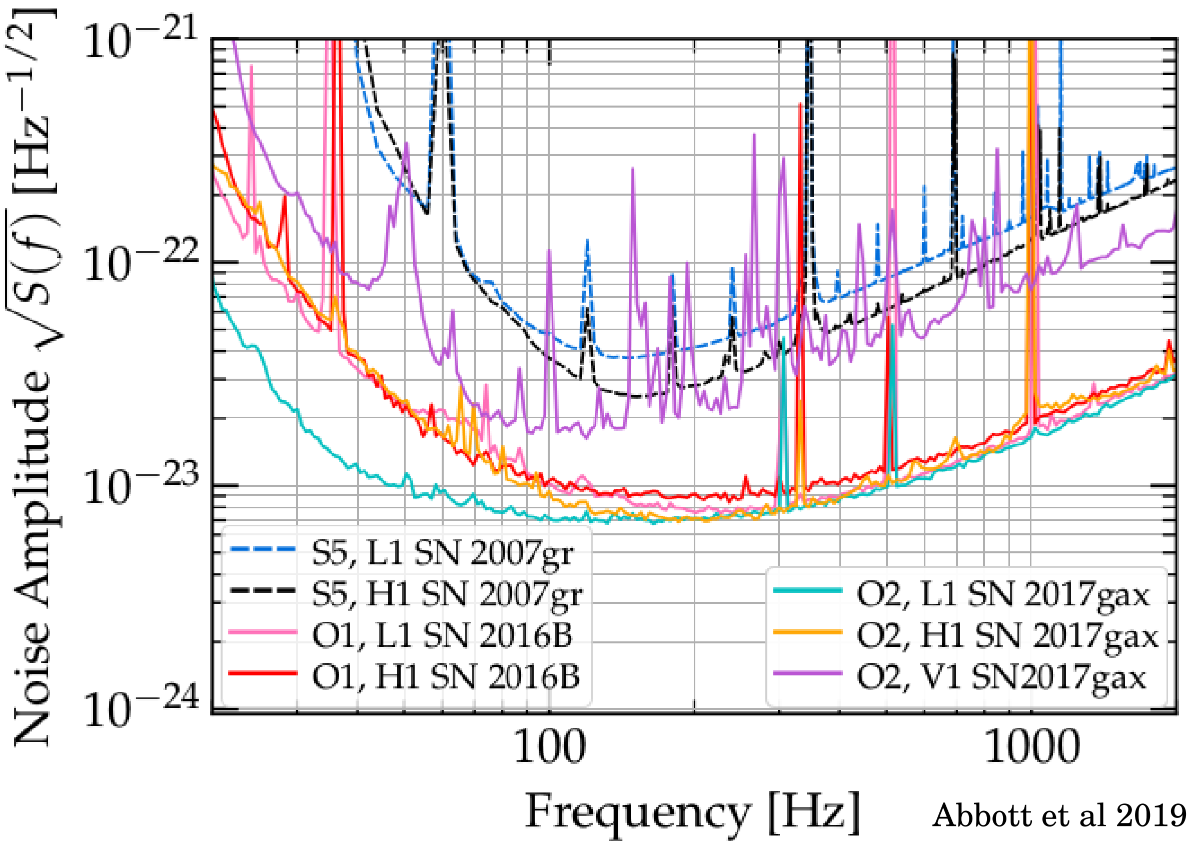

Abbott et al 2019

- Periods of poor data quality are excluded
- L1 and H1 detector improvements between O1-O2 and S5-S6:
  - around 3-5 times more sensitive between 100 Hz and 300 Hz
  - around 10 times more sensitive around 1 kHz
- V1 was excluded from the analysis, H1L1V1 network is less sensitive than H1L1 network

Methodology

- Search pipeline **Coherent WaveBurst** (Klimenko et al 2016)
  - Constrained maximum likelihood
  - **Ranking statistics**: $\rho \propto \sqrt{E_c}$, where E_c is the normalized coherent energy obtained by cross-correlating the reconstructed waveforms in each detector
  - Correlation coefficient, *cc,* measures degree of similarity of the waveforms between the detectors (real GW, cc~1, search cut cc>0.8)
- **Search bandwidth: 16-2048 Hz**
- Search classes:
  - class C1 – transients of a few cycles (e.g. blips)
  - class C2 – other noise transients
- **Loudest event statistics**
- **Background estimation**, *events significance*: $\mathrm{FAP} = 1 - \exp\left(-T_{\mathrm{coinc}} \times \mathrm{FAR}\right)$

  (False Alarm Probability and Rate (FAP and FAR), T_{coinc} – coincident duty factor)
- **Search sensitivity**: cWB adds (injects) to data CCSN waveforms, performs analysis and fraction of detected events we call *detection efficiency*

CCSN waveforms

	Waveform Family	Waveform Identifier	$h_{\rm rss}$ $[10^{-22}\sqrt{\rm s}$ @10 kpc]	$f_{\rm peak}$ [Hz]	$E_{\rm GW}$ $[10^{-9} M_\odot c^2]$	Polarizations
Neutrino-driven explosions	Müller [91] 3D Convection and SASI	mul1-L15-3	1.655	150	3.741×10^{-2}	+, ×
		mul2-N20-2	3.852	176	4.370×10^{-2}	+, ×
		mul3-W15-4	1.093	204	3.247×10^{-2}	+, ×
	Ott [92] 3D Convection and SASI	ott1-s27fheat1p05	0.238	1019	7.342×10^{-1}	+, ×
	Yakunin [93] 2D Convection and SASI	yak1-B12-WH07	3.092	760	3.411	+
		yak2-B15-WH07	14.16	932	7.966	+
		yak3-B20-WH07	3.244	638	4.185	+
		yak4-B25-WH07	18.05	1030	14.21	+
MHD-driven explosions	Scheidegger [94] Rotating Core-Collapse	sch1-R1E1CA$_L$	0.129	1155	1.509×10^{-1}	+, ×
		sch2-R3E1AC$_L$	5.144	466	2.249×10^{2}	+, ×
		sch3-R4E1FC$_L$	5.796	698	4.023×10^{2}	+, ×
	Dimmelmeier [95] Rotating Core-Collapse	dim1-s15A2O05ls	1.052	770	7.685	+
		dim2-s15A2O09ls	1.803	754	27.880	+
		dim3-s15A3O15ls	2.690	237	1.380	+
Extreme emission models	Long-lasting Bar Mode [100]	lb1-M0.2L60R10f400t100	1.480	800	2.984×10^{-4}	+, ×
		lb2-M0.2L60R10f400t1000	4.682	800	2.979×10^{-3}	+, ×
		lb3-M0.2L60R10f800t100	5.920	1600	1.902×10^{-2}	+, ×
		lb4-M1.0L60R10f400t100	7.398	800	7.459×10^{-3}	+, ×
		lb5-M1.0L60R10f400t1000	23.411	800	7.448×10^{-2}	+, ×
		lb6-M1.0L60R10f800t25	14.777	1601	1.184×10^{-1}	+, ×
	Torus Fragmentation Instability [101]	piro1-M5.0η0.3	2.550	2035	6.773×10^{-4}	+, ×
		piro2-M5.0η0.6	9.936	1987	1.027×10^{-2}	+, ×
		piro3-M10.0η0.3	7.208	2033	4.988×10^{-3}	+, ×
		piro4-M10.0η0.6	28.084	2041	7.450×10^{-2}	+, ×
Ad-hoc waveforms	sine-Gaussian [31]	sg1-235HzQ8d9linear	—	235	—	+
		sg2-1304HzQ8d9linear	—	1304	—	+
		sg3-235HzQ8d9elliptical	—	235	—	+, ×
		sg4-1304HzQ8d9elliptical	—	1304	—	+, ×

Results – Loudest Events

- The non negligible values of the FAP indicate that all the loudest events appear compatible with the noise background.
- Results of the search (loudest event statistics):
  - Detection efficiencies
  - GW energy constraints
  - Extreme emission model exclusion statements

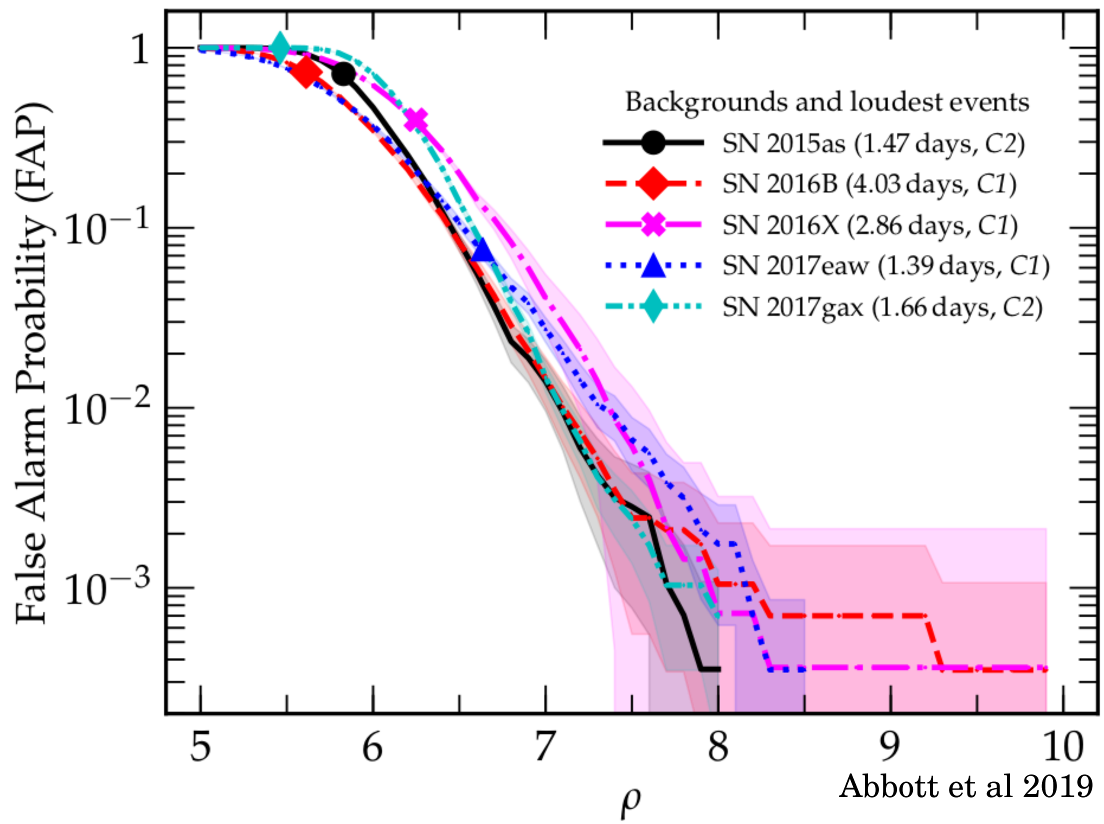

Abbott et al 2019

Supernova	Class	ρ	FAR [Hz]	FAP
SN 2015as	*C2*	5.8	2.9×10^{-5}	0.716
SN 2016B	*C1*	5.6	1.1×10^{-5}	0.732
SN 2016X	*C1*	6.2	1.4×10^{-5}	0.398
SN 2017eaw	*C1*	6.6	1.3×10^{-6}	0.076
SN 2017gax	*C2*	5.5	9.7×10^{-5}	1.000

Results – Detection Efficiencies

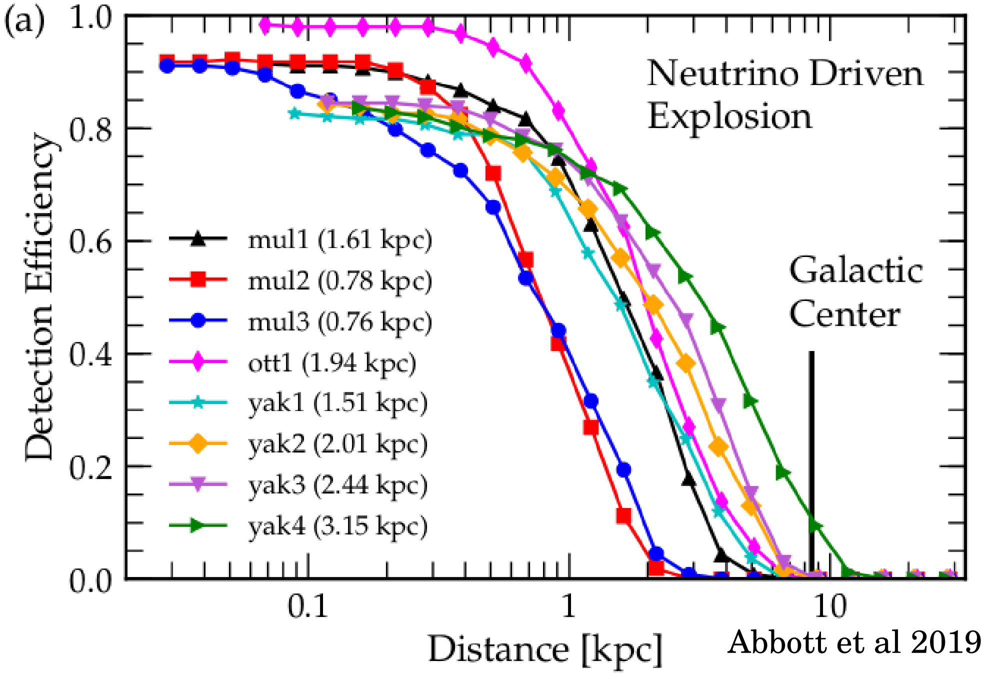

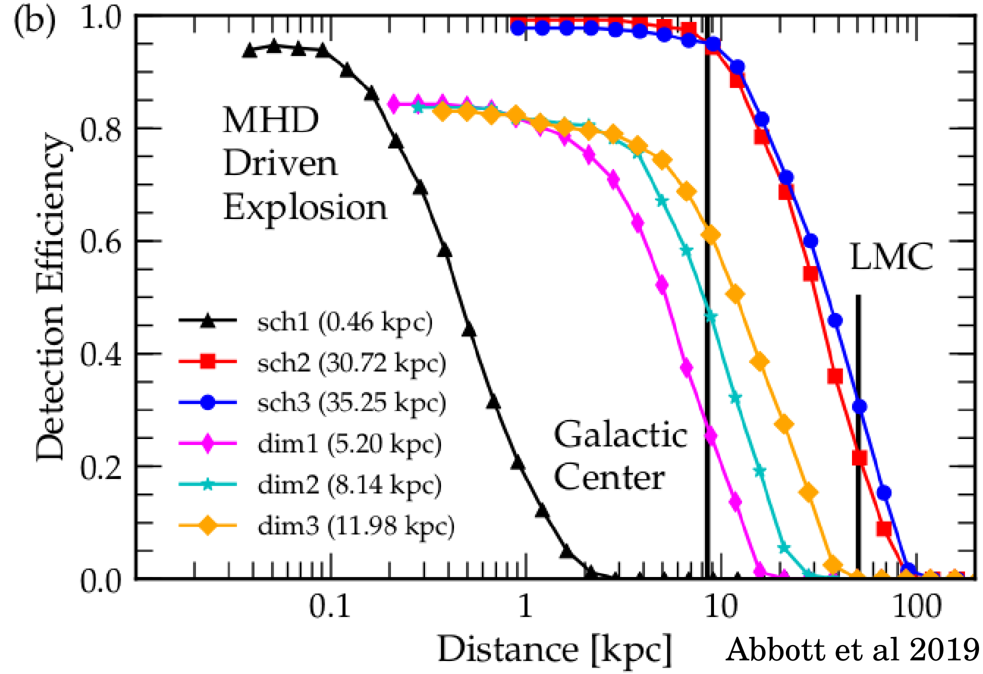

- We accept events more significant than the loudest events
- Example plot: SN 2017eaw (6.7 Mpc)
- Detection ranges for SN 2017gax (19.7 Mpc):
  - 5 kpc (neutrino-driven explosions),
  - 54 kpc (MHD-driven explosions)
- Detection ranges improvement correspond to detectors improvement between S5-S6 and O1-O2 runs.

Results – Detection Efficiencies

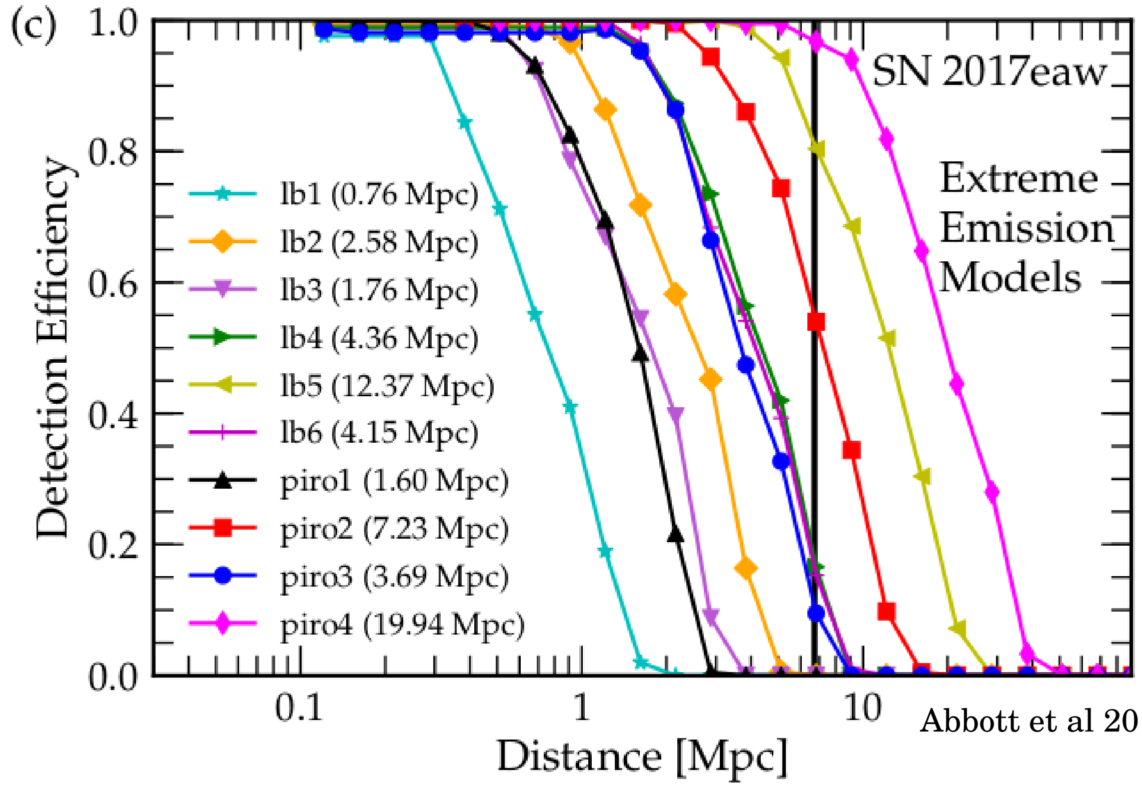

Abbott et al 2019

- We accept events more significant than the loudest events
- Example plot: SN 2017eaw (6.7 Mpc)
- Detection ranges for SN 2017gax (19.7 Mpc): 28 Mpc
- Given non-zero detection efficiencies for extreme emission models, we exclude parameter spaces of these models.

Results – Model Exclusion

- **For the first time, the gravitational-wave data enabled us to exclude parameter spaces of two extreme emission models.**
- These results are consistent with the current theoretical understanding
- We combine 5 supernovae in a standard candle approach
- Reduced detection efficiency – model exclusion probability $\epsilon(d)$
- Overall model exclusion probability P_{excl}:

$$P_{\text{excl}} = 1 - \prod_{i=1}^{N} (1 - \epsilon_i(d_i))$$

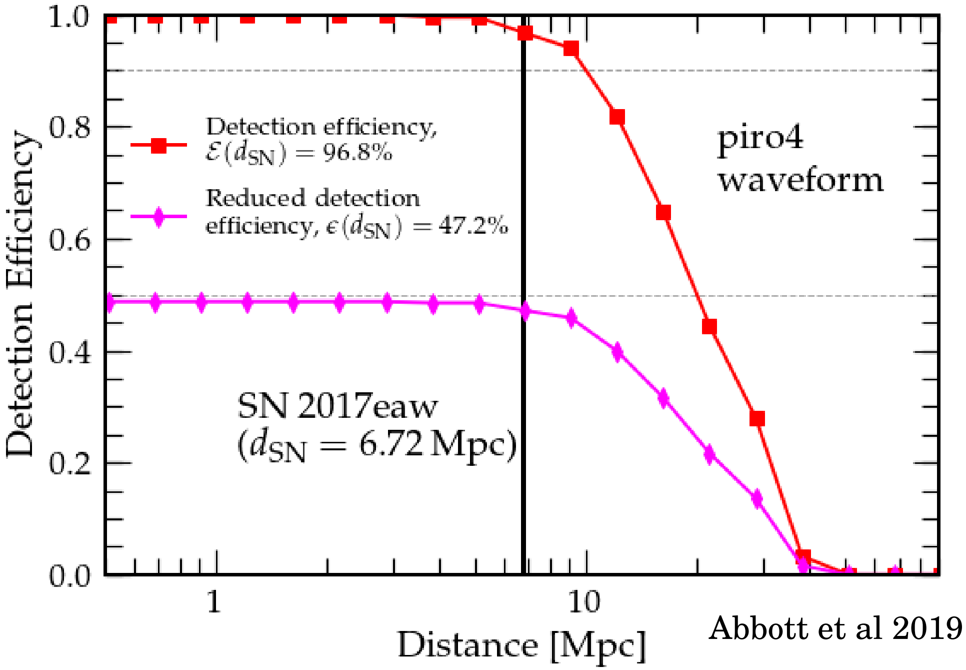

Abbott et al 2019

Supernova		piro1	piro2	piro3	piro4	lb1	lb2	lb3	lb4	lb5	lb6
Reduced Detection Efficiency ϵ [%]	SN 2015as	0.0	0.2	0.0	18.0	0.0	0.0	0.0	0.0	8.4	0.0
	SN 2016B	0.0	0.1	0.0	16.0	0.0	0.0	0.0	0.0	5.5	0.0
	SN 2016X	0.0	0.0	0.0	9.8	0.0	0.0	0.0	0.0	3.1	0.0
	SN 2017eaw	0.0	26.8	5.2	47.2	0.0	0.0	0.0	8.7	39.5	8.0
	SN 2017gax	0.0	0.2	0.0	48.7	0.0	0.0	0.0	0.0	28.6	0.0
P_{excl} [%]		0.0	**27.2**	**5.2**	**83.2**	0.0	0.0	0.0	**8.7**	**63.8**	**8.0**

Results – Model Exclusion

- **Long-Lasting Bar Mode instability**:
  - Creation of bars due to rapid rotation
  - The deformations are preferably small: 2R<20km and L/2R<2.5, or 2R≈40km and L/2R≤1.5–3.5.
  - The deformations are preferably short lived, less than 1s: 2R<20km and L/2R>3.

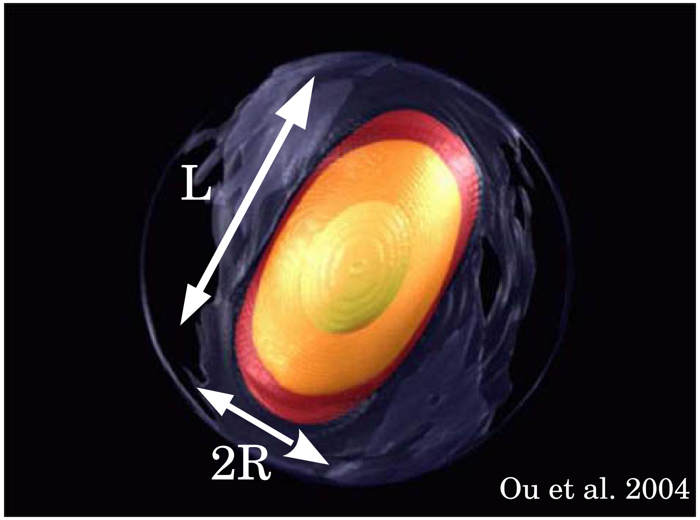

- **Torus Fragmentation instability** (Piro&Pfahl 2007):
  - Black Hole (BH) is formed in the center and fragmented clump of matter accretes into BH
  - The clump of matter is preferably small $M_f << M_\odot$
  - Tori around central BH are non-fragmented or thin

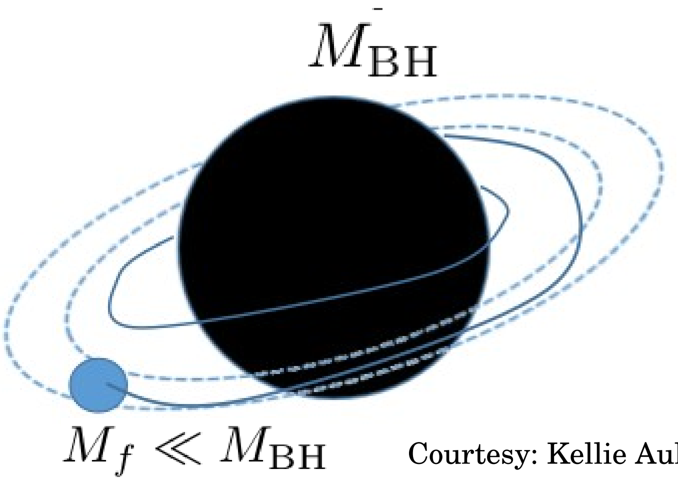

Courtesy: Kellie Ault

Results – GW Energy Constraints

- Constraint on the GW energy emitted by a CCSN source
- Isotropic emission assumed:

$$E_{\rm GW} = \frac{\pi^2 c^3}{G} D^2 f_0^2 h_{\rm rss}^2$$

where D – distance to the CCSN, f_0 – peak frequency

- Root-mean-square:

$$h_{\rm rss} = \sqrt{\int \langle h_+^2(t) + h_\times^2(t)\rangle_\Omega \, dt}$$

- Ad-hoc sine-Gaussian waveforms with duration:

$$\tau = Q/(\sqrt{2}\pi f_0)$$

where Q=8.9 is quality factor.

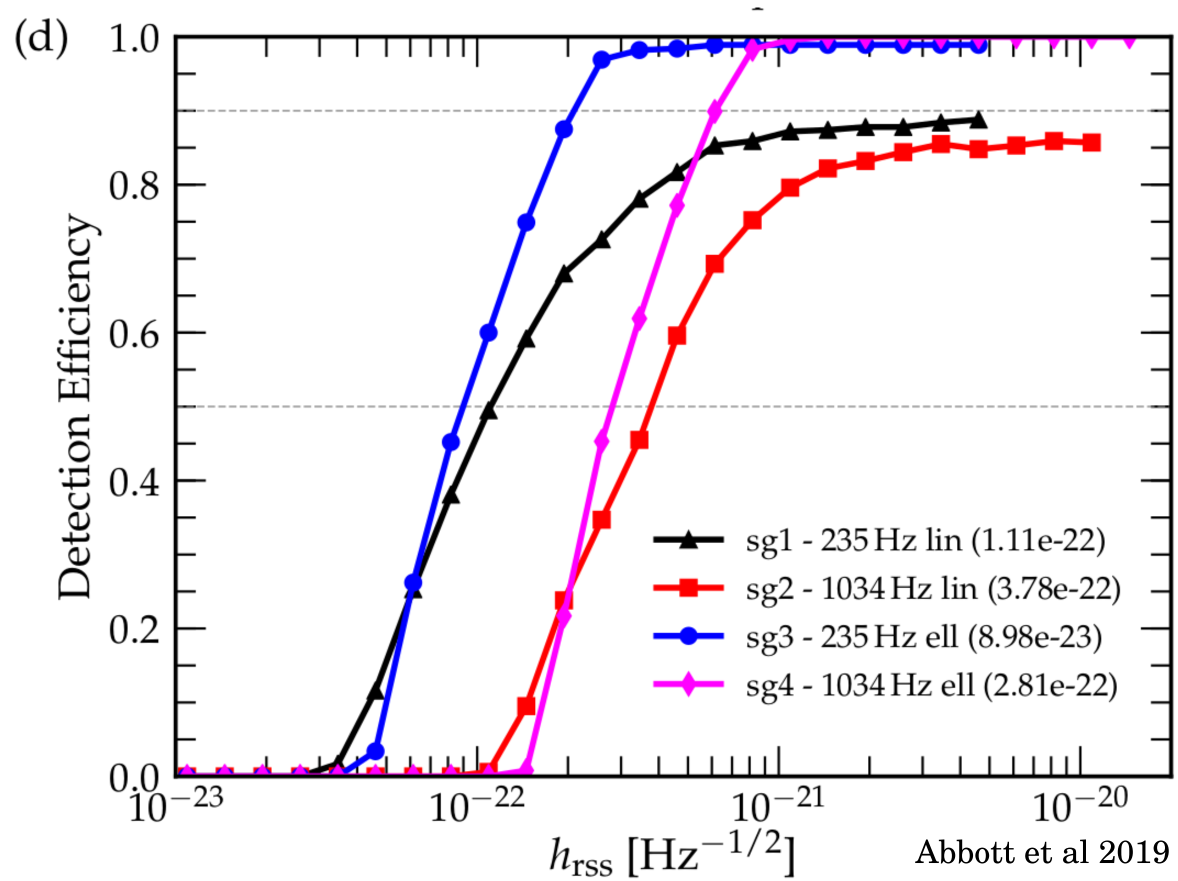

Abbott et al 2019

Results – GW Energy Constraints

- iLIGO SN Search E_{GW} constraints: 5.8x10^{-2} $M_{\odot}c^2$ (235Hz) and 26 $M_{\odot}c^2$ (1304 Hz)
- Typical explosion energy (~10^{51} erg) and typical kinetic energy of the ejecta (~10^{51} erg)

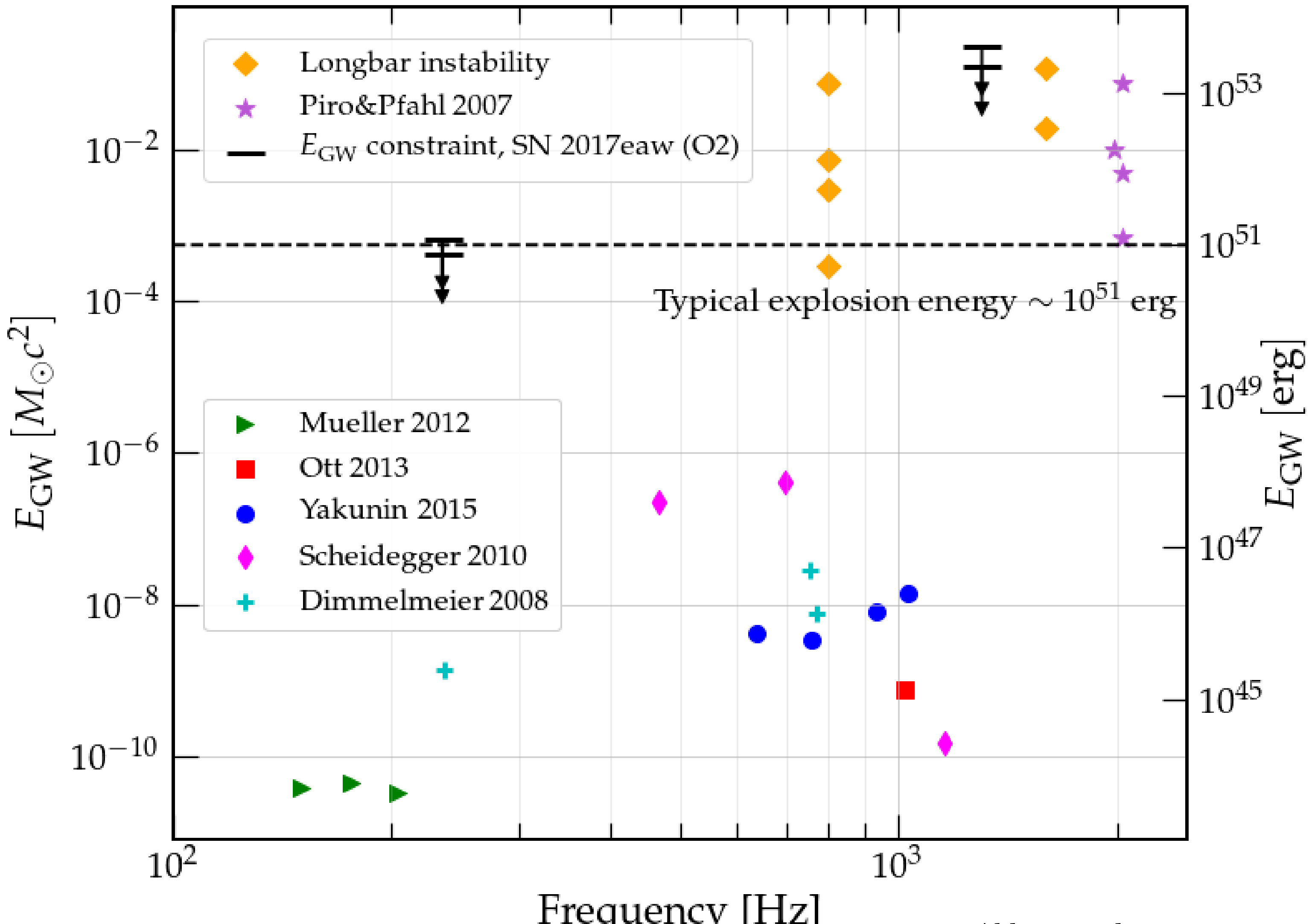

Abbott et al 2019

Summary

- No significant GW candidate
- Detection ranges up to 5 kpc for neutrino-driven explosions
- Model exclusion for two extreme emission models up to 83% confidence
- GW energy constraints down to ~10^{-3} $M_{\odot}c^2$